3-port polarization-independent optical quasi-circulator with holographic spatial walk-off polarizers

Jing-Heng Chen, Kung-Huang Chen, Po-Jen Hsieh, and Der-Chin Su
Institute of Electro-Optical Engineering,
National Chiao Tung University, 1001 Ta-Hsueh Road, Hsin-Chu 30050, Taiwan, R.O.C.

ABSTRACT

An alternative type of 3-port polarization-independent optical quasi-circulator by utilizing a pair of holographic spatial walk-off polarizers (HSWPs) is proposed. This device consists of a reflection prism, three polarization beamsplitter cubes, a pair of HSWPs, a Faraday rotator, and a half-wave plate. The operating principles, the characteristics, and the performances of this device and HSWPs are discussed. In order to show the validity, the prototype device operating in 1300nm is assembled and tested experimentally. The merits of this design include polarization-independence, compactness, high isolation, and easy fabrication. It should also be possible to design the device operating at 1550 nm wavelength range.

Keywords: Optical communications, Holographic optical elements, Polarization

1. INTRODUCTION

Optical circulators[1-5] are important nonreciprocal devices that direct a light from one port to another sequentially in only one direction. Circulators are necessary components in the construction of fundamental network modules such as optical add/drop multiplexers[6, 7], dispersion-compensation[8], optical amplifiers[7], and time-domain reflectometry[9]. Several types of circulator design had been proposed[2-5] that use spatial walk-off polarizers (SWPs) to manipulate the polarized components of incident light. The conventional SWPs[10, 11] made of birefringent crystals capable of splitting an optical beam into two orthogonally polarized parallel beams. However, the conventional birefringent crystals suffer from the challenge of high optical qualities, crystal manufacturing, and hard optical fabrications. So the cost may be too high. In addition, the separation between the two orthogonally polarized beams produced by the conventional crystals is typically limited by the small birefringence. A volume holographic grating has special functions and high efficiency, so it is always used as an alternative element, especially in the category[12, 13] of optical communications. In this paper, we propose a holographic spatial walk-off polarizer (HSWP) to replace the crystal type SWP. To demonstrate the feasibility of the idea, some sample HSWPs are designed by using the coupled-wave theory[14] and fabricated with the conventional holographic recording geometry under the conditions derived from Chen's corrected methodology[15]. The HSWPs are designed for the 1300nm wavelength and were fabricated with an He-Cd laser at the wavelength of 441.6nm and with the dichromated gelatin (DCG) as the recording material[16, 17]. The fabricated HSWPs have a larger splitting angle of 60° and the demonstrated diffraction efficiencies of the s- and p- polarized components are 3% and 90% respectively, limited by our experimental conditions. With a pair of our fabricated HSWPs, a new type of 3-port polarization-independent optical quasi-circulator is designed by modifying the configuration of Nicholls[11]. The characteristics of the HSWPs as well as the operating principle and the performance of the proposed optical quasi-circulator will be discussed in the following sections.

2. DESIGN OF 3-PORT POLARIZATION-INDEPENDENT OPTICAL QUASI-CIRCULATOR

This alternative type of 3-port polarization-independent optical quasi-circulator with a pair of HSWPs is designed, as shown in Fig. 1. The HSWPs are used to replace the crystal type SWP. Besides the HSWPs, this optical circulator consists of a reflection prism (RPs), three polarization-beam splitters (PBSs), a 45° Faraday rotator (FR), and a 45° half-wave plate (H). The two identical HSWPs face the opposite directions as shown in the figure. If an input beam is

Reliability of Optical Fiber Components, Devices, Systems, and Networks II,
edited by Hans G. Limberger, M. John Matthewson, Proc. of SPIE Vol. 5465
(SPIE, Bellingham, WA, 2004) · 0277-786X/04/$15 · doi: 10.1117/12.544488

normally incident on $HSWP_1$ from Port 1 as shown in Fig. 1(a), then the s- polarized component passes through $HSWP_1$ directly and the p- polarized component also passes through $HSWP_1$ after two diffractions and two total-reflections. Next, these two orthogonally polarized components pass through FR and H. Their states of polarization (SOP) are rotated a total of 90°, +45° by FR and +45° by H. For easy understanding, a circle with a bisecting line is used to represent the associated SOP of the light after propagating through each component. Symbols ⦶ and ⊖ represent the electric-field lies in the planes perpendicular (s-polarization) and parallel (p-polarization) to the paper plane respectively, and the symbol ⊕ represents the light beam has both s- and p- polarized components. The beams finally enter $HSWP_2$ and then recombine together with the similar diffraction and total-reflection effects in $HSWP_1$ and reach Port 2.

On the other hand, if an input beam is incident normally on $HSWP_2$ from Port 2 as shown in Fig. 1(b), then the s-polarized component passes through $HSWP_2$ directly, and the p- polarized component also passes through $HSWP_2$ after two diffractions and two total-reflections. These two orthogonally polarized components pass through H and FR. Their SOPs are rotated -45° by H and +45° by FR, a total of 0°. The s- polarized component passes through $HSWP_1$ and is reflected by three PBSs and enters Port 3. The p- polarized component is diffracted and total-reflected similarly in $HSWP_1$ and propagates through one RP, and one PBS. Finally, it arrives at Port 3 and recombines with the s- polarized component. If the PBSs are located accurately in the configurations of Fig. 1(b), there will be no optical path difference between s- and p- polarizations for the route of Port 2→Port 3. Hence, this optical circulator can function as a polarization-independent 3-port optical quasi-circulator without polarization mode dispersion (PMD).

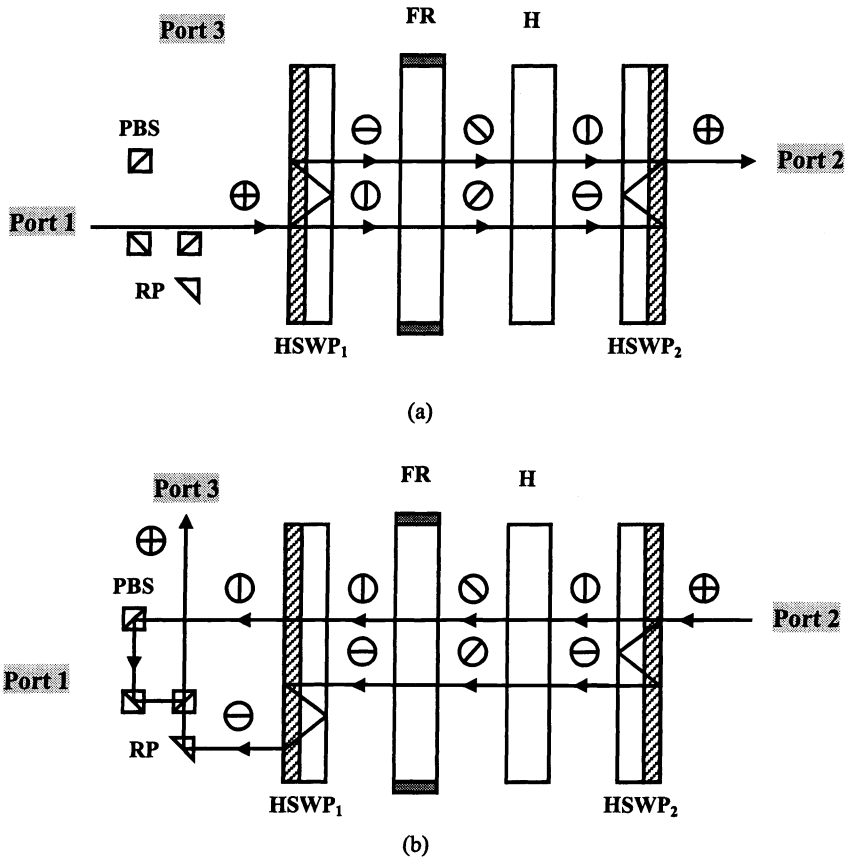

Fig. 3. Structure and operation principles of the proposed 3-port polarization independent optical quasi-circulator.

3. HOLOGRAPHIC SPATIAL WALK-OFF POLARIZER

The holographic spatial walk-off polarizer (HSWP) is a transmission-type phase volume holographic grating on a substrate, as shown in Fig. 2. In order to replace the function of conventional SWPs, its grating structure is designed in such a way that the s- polarized component of a normal incident beam at A is transmitted straight through the grating and the substrate while the p- polarized component is completely diffracted into the substrate with a diffraction angle θ_{s2} which is larger than the critical angle θ_c at the substrate-air interface. In this way, the diffracted beam is totally reflected at point B and hits the grating again at point C. This beam is totally reflected at point C, and the reflected beam from point C satisfies the Bragg condition[14] of the grating. The propagation direction of the reflected beam is in parallel to that of the beam diffracted by the grating at point A. Because the structure of the grating at point C is the same as that at point A, the diffracted beam at point C will be in parallel to the input beam at point A; that is, the output beam passes normally through the substrate. The detail of the beam propagation at point C is shown in the upper left circle of Fig. 2. Consequently, two orthogonally polarized parallel beams with the separation of length AC can be obtained.

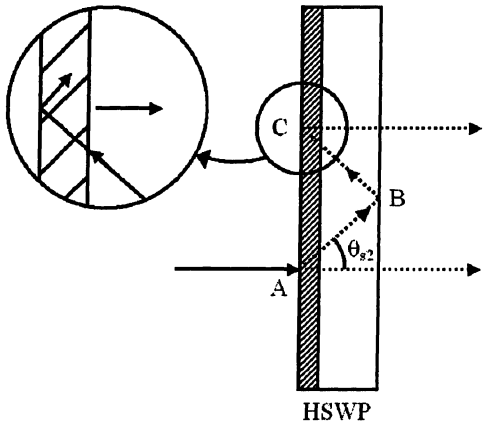

Fig. 2. Structure and operation principle of the holographic spatial walk-off polarizer.

3.1 Diffraction efficiency of an HSWP

Because the incident angle of the input beam is set to be 0, the diffraction efficiencies of this grating for s- and p-polarized components can be derived from the coupled-wave theory[14] and can be respectively written as

$$\eta_s = \sin^2\left[\frac{\pi n_1 d}{\lambda_r}\frac{1}{(\cos\theta_d)^{1/2}}\right] = \sin^2 \upsilon_s, \tag{1}$$

and

$$\eta_p = \sin^2\left[\frac{\pi n_1 d}{\lambda_r}\frac{1}{(\cos\theta_d)^{1/2}}\cos\theta_d\right] \tag{2}$$
$$= \sin^2(\upsilon_s \cos\theta_d) = \sin^2 \upsilon_p.$$

Here θ_d is the diffraction angle in the phase volume grating, n_1 is the index modulation strength, d is the hologram emulsion thickness, and λ_r is the reconstruction wavelength. For our applications, the necessary condition for this grating to satisfy is that η_p is 100% and η_s is zero.

3.2 Optical recording and reconstruction geometry

The optical configuration for recording and reconstructing the transmission-type phase volume holographic grating is shown in Fig. 3. Two light beams R_1 and S_1 with wavelength λ are incident on a recording material at θ_{r1} and θ_{s1}. The recording material consists of a substrate and a photographic emulsion with refractive index n_{f1} (at λ) and thickness d_1. After the exposure, the recording material is post-processed for developing. The thickness of the photographic emulsion shrinks to d after developing. The reconstructed light R_2 with wavelength λ_r is incident normally (i.e. $\theta_{r2}=0°$), and the outgoing wave S_2 with diffracted angle $\theta_{s2} = \sin^{-1}[\frac{n_{f2}}{n_s}\sin\theta_d]$ in the substrate. Here n_s and n_{f2} are the refractive indices of the substrate and the processed photographic emulsion at λ_r, respectively. Considering the emulsion shrinkage and average refraction index shift, the K-vector diagram[14] is shown in Fig. 4, where K_1 and K_2 are the grating vectors before and after post-processing, respectively. The values of the recording conditions θ_{r1} and θ_{s1} can be calculated by using Chen's corrected methodology[15] under the experimental conditions in which λ, λ_r, n_{f1}, d_1, n_{f2}, d, θ_{r2} and θ_{s2} are specified.

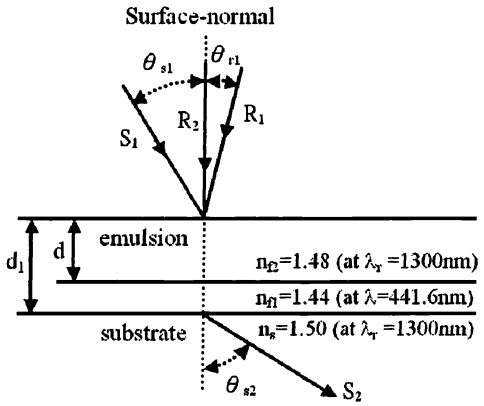

Fig. 3 Geometry for recording and reconstruction the transmission-type phase volume holographic grating considering the thickness and refractive index shifts after optical exposure and post-processing.

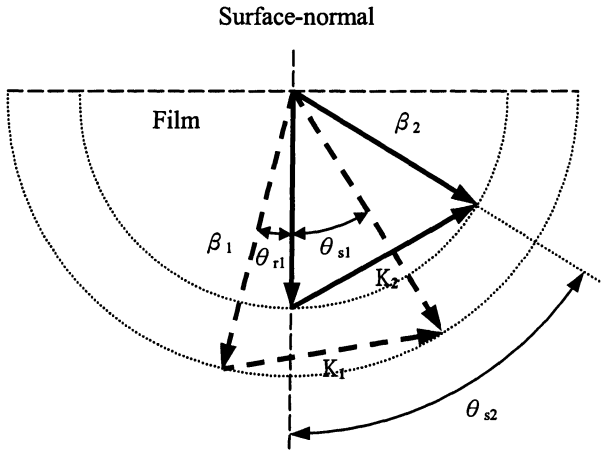

Fig. 4 K-vector diagram of shorter-wavelength construction for longer-wavelength reconstruction.

4. FABRICATIONS RESULTS AND DISCUSSIONS

In order to demonstrate the validity of our design, several HSWPs for 1300 nm wavelength are fabricated. An He-Cd laser with wavelength λ =441.6 nm is used for exposure and the dichromated gelatin (DCG) is used as the recording material. We prepare the DCG recording material with the processes proposed by McCauley et al.[17]. Since in general it is difficult to fabricate DCG with $n_1 > 0.08$[16], so we first substitute the specifications d=17μm and n_1<0.08, $\theta_{s2}>\theta_c$ ($\fallingdotseq$41.8°), and λ_r=1300nm into Eqs. (1) and (2) under the necessary condition described in **Sec. 3.1**. The results we get are θ_d=60° and n_1=0.054. Fig. 5 shows the calculated curves of diffraction efficiency versus index modulation strength for s- and p- polarizations in our experimental conditions. Next, the recording conditions θ_{r1}=14.1° and θ_{s1}=32.6° are obtained by substituting the experimental conditions λ=441.6nm, λ_r=1300nm, d_1=22μm, n_{f1}=1.44 (at λ=441.6nm), d=17μm, n_{f2}=1.48 (at λ_r=1300nm), θ_{r2}=0°, and θ_{s2}=58.7° (i. e. θ_d=60°) into Chen's corrected methodology. After exposure and post-processing, the HSWPs are obtained and their diffraction efficiencies are measured to be η_s=3% and η_p=90%. The separation between the two orthogonally parallel beams is 3.2 mm.

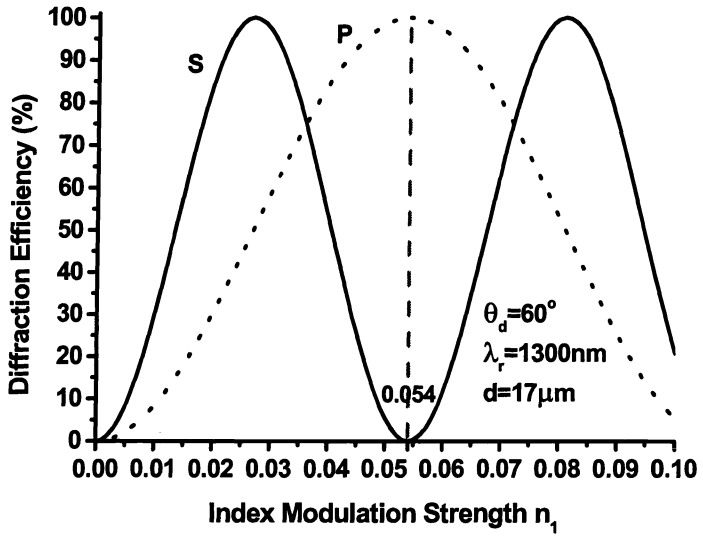

Fig. 5 Calculated relation curves of diffraction efficiency versus index modulation strength for s- and p- polarizations.

Furthermore, a prototype of the 3-port optical circulator for 1300nm is assembled with a pair of our fabricated HSWPs, a Faraday rotator and a half wave-plate. In addition, it needs another three polarization-beam splitters and one reflection prism to complete the function of this 3-port optical quasi-circulator.

The characteristic parameters of this prototype device can be estimated from that of each component. The diffraction efficiencies of HSWPs, as mentioned above, are measured to be η_s=3% and η_p=90%. The transmittances of FR and H, which are commercial devices, are listed to be 0.95 and 0.97, respectively. Thus, the associated losses and isolation values of this optical quasi-circulator can be estimated, as shown in Table 1(a). In order to confirm the validity of this estimation, we have measured the insertion losses of the device. The measured values are correspondent well with the estimated values. Because η_s and η_p of our fabricated HSWPs are slightly different from the theoretical values, the transmittances of two orthogonally polarized components are slightly different in the route of Port 2→Port 3.

If our fabricated HSWPs are anti-reflection coated and are under accurate fabrication processes, the reflection losses should be decreased to 0.1%, and the diffraction efficiencies may reach theoretical values[18], i.e., $\eta_s \fallingdotseq 0\%$ and $\eta_p \fallingdotseq$ 100%. Under these two improved conditions, the performance of this 3-port optical quasi-circulator can be enhanced greatly, and the associated parameters are calculated and listed in Table 1(b) with η_s<1% and η_p>99%.

Table 1. Associated losses and isolation values[a] (in Decibels) of the 3-port optical quasi-circulator with wavelength 1300nm by using (a) our fabricated HSWPs; and (b) ideal HSWPs with anti-reflection coatings and diffraction efficiencies of η_s<1% and η_p>99%.

(a)

	Out Port		
In Port	**1**	**2**	**3**
1	14.26[b]	2.09[c]	47.91
2	11.91	14.26[b]	2.02[c]

(b)

	Out Port		
In Port	**1**	**2**	**3**
1	>30[b]	<0.50[c]	>73.06
2	>20.42	>30[b]	<0.50[c]

[a]All values without a superscript are isolation values;
[b]Return losses;
[c]Insertion losses.

Moreover, if K and $\Delta\lambda$ are the magnitude of grating vector $\vec{K}$ and the wavelength shift with respect to the central wavelength λ_r, the diffraction efficiencies of a transmission-type phase volume hologram for the s- and p-polarization states near the Bragg condition are given as[14]

$$\eta_i = \frac{\sin^2(\sqrt{\nu_i^2 + \xi^2})}{(1 + \xi^2 / \nu_i^2)} \quad (i = s,p), \tag{3}$$

with

$$\xi = \frac{-\Delta\lambda K^2 d}{8\pi n_{f2} \cos\theta_d}, \tag{4a}$$

$$K = (\frac{4\pi n_{f2}}{\lambda_r}) \cdot \sin\frac{\theta_d}{2}. \tag{4b}$$

Substituting our experimental conditions n_1=0.054, d=17μm, λ_r=1300nm, θ_d=60°, and n_{f2}=1.48 (at λ_r=1300nm) into Eq. (3), the theoretical curves of diffraction efficiencies versus wavelengths for our HSWP is shown in Fig. 6. It is obvious that the bandwidth with η_p>90% and η_s≅0% at 1300nm central wavelength is as large as 20nm. It should also be possible to design the central wavelength to be at 1550 nm wavelength range.

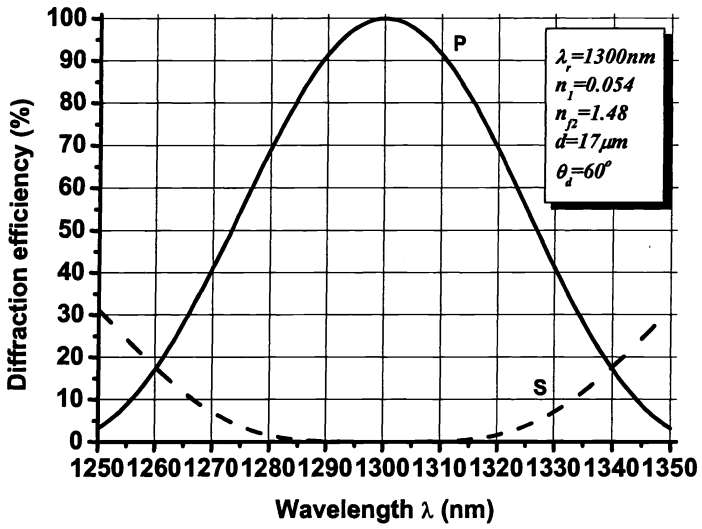

Fig. 6 Calculated diffraction efficiencies of the HSWP versus wavelength at 1300nm central wavelength.

5. CONCLUSIONS

An alternative type of 3-port polarization-independent optical quasi-circulator by using a pair of holographic spatial walk-off polarizers (HSWPs) has been proposed. In order to demonstrate the feasibility, the prototype of a 3-port optical quasi-circulator operating at a wavelength of 1300nm was assembled. In addition, the operating principles and the performance of the proposed optical quasi-circulator have been described. This design has advantages of polarization-independence, compactness, high isolation, and easy fabrication. It should also be possible to design the device operating at 1550 nm wavelength range.

ACKNOLEGEMENTS

This research were supported partially by grants from the National Science Council of ROC under contract No. NSC-92-2215-E-009-052, and the Lee & MTI Center for Networking at the National Chiao Tung University, Taiwan, R. O. C.

REFERENCES

1. J. Hecht, *Understanding fiber optics* (Prentice Hall, New Jersey, 2002), Chap. 14.
2. J. H. Chen et al. "Holographic spatial walk-off polarizer and its application to a 4-port polarization-independent optical circulator," Optics Express **11**, pp. 2001-2006, 2003.
3. N. Sugimoto et al. "Waveguide polarization-independent optical circulator," IEEE Photon. Technol. Lett. **11**, pp. 355-357, 1999.
4. L. D. Wang, "High-isolation polarization-independent optical quasi-circulator with a simple structure," Opt. Lett. **23**, pp. 549-551, 1998.
5. M. Koga, "Compact quartzless optical quasi-circulator," Electron. Lett. **30**, pp. 1438-1440, 1994.
6. Y. K. Chen et al. "Low-crosstalk and compact optical add-drop multiplexer using a multiport circulator and fiber Bragg gratings," IEEE Photon. Technol. Lett. **12**, pp. 1394-1396, 2000.
7. A. V. Tran et al. "A bidirectional optical add-drop multiplexer with gain using multiport circulators, fiber Bragg

gratings, and a single unidirectional optical amplifier," IEEE Photon. Technol. Lett. **15**, pp. 975-977, 2003.
8. D. K. Mynbaev, and L. L. Scheiner, *Fiber-optic communications technology* (Prentice Hall, New Jersey, 2001), Chap. 6.
9. Y. Sato and K. Aoyama, "OTDR in optical transmission systems using Er-doped fiber amplifiers containing optical circulators," IEEE Photon. Technol. Lett. **3**, pp. 1001-1003, 1991.
10. R. Ramaswami, K. N. Sivarajan, *Optical networks*, second ed., Morgan Kaufmann, San Francisco, 2002, pp. 112-115 (Chapter 3).
11. J. Nicholls, "Birefringent crystals find new niche in WDM networks," WDM SOLUTIONS **3,** pp. 33-36, 2001.
12. J. Liu and R. T. Chen, "Path-reversed substrate-guided-wave optical interconnects for wavelength-division demultiplexing," Appl. Opt. **38**, pp. 3046-3052, 1999.
13. R. Shechter, Y. Amitai, and A. A. Friesem, "Compact wavelength division multiplexers and demultiplexers," Appl. Opt. **41**, pp. 1256-1261, 2002.
14. H. Kogelnik, "Coupled wave theory for thick hologram gratings," Bell Syst. Tech. J. **48**, pp. 2909-2947, 1969.
15. J. H. Chen, D. C. Su, J. C. Su, "Shrinkage- and refractive-index shift-corrected volume holograms for optical interconnects," Appl. Phys. Lett. **81**, pp. 1387-1389, 2002.
16. B. J. Chang, C. D. Leonard, "Dichromated gelatin for the fabrication of holographic optical elements," Appl. Opt. **18**, pp. 2407-2417, 1979.
17. D. G. McCauley, C. E. Simpson, W. J. Murbach, "Holographic optical element for visual display applications," Appl. Opt. **12**, pp. 232-242, 1973.
18. B. J. Chang, Optical information storage, Proc. SPIE, vol. **177**, pp. 71-81, 1979.